Tea Polyphenol EGCG Increases Nanoplastics Release from Plastic Cups but Mitigates Potential Detrimental Effects

*Haoxin Ye[a], David D. Kitts[a], Xiwen Wang[a], Yifan Wang[a] and Tianxi Yang[a]**

a Food, Nutrition and Health, Faculty of Land and Food Systems, The University of British Columbia, Vancouver V6T1Z4, Canada

***Corresponding author: Tianxi Yang (tianxi.yang@ubc.ca)**

ABSTRACT

The presence of micro/nanoplastics in ecosystems and the potential for carry-over into daily human routines poses huge human health risks. While MNPs released from plastic packaging materials at different environmental conditions (e.g., pH, temperature) have been explored, the influence of real food ingredients (e.g., polyphenols) on plastic release has not been studied. Herein, for the first time, we investigated the effect of epigallocatechin gallate (EGCG), a relevant catechin polyphenol common to tea, on the release of nanoplastics from polystyrene (PS) cups during a heating process. We developed a novel surface-enhance Raman scattering sensor to quantify released nanoplastics *in situ* using EGCG-based luminescent metal phenolic network labeling strategies. The presence of added EGCG enhanced MNP release ($P<0.05$) when microwaved, more so than in boiling water relative to cold water control. We also observed that the higher amounts of added EGCG at the same pH and temperature caused higher amounts of nanoplastics due to the interaction of EGCG with nanoplastics. Reusing PS cups treated with EGCG in boiling water resulted in a gradual increase in nanoplastic release over 4 cycles. Of interest was the finding that EGCG also mitigated the detrimental effects of increased nanoplastics exposure in differentiated Caco-2 cell redox status in a concentration-dependent manner ($P<0.05$). These results imply that polyphenols as food and beverage ingredients may influence exposure to nanoplastics, but also may act to reduce nanoplastic cytotoxicity. This finding underlines the importance of broader consideration of food safety in public health discussions, focusing particularly on the composition of the food matrix and food processing and packaging applications that relate to different foods.

KEYWORDS: Nanoplastics release; epigallocatechin gallate; luminescent metal–phenolic networks; SERS, nanoplastics detrimental effects

INTRODUCTION

The practice of using plastics in many aspects of consumer daily activities, ranging from purchasing clothing and healthcare products to also including a variety of packaged food products to increase shelf-life and safety, is an ongoing reality. The omnipresence of micro/nanoplastics (MNPs) has resulted in increased awareness of the consequences to ecological and environmental issues that relate to pollution of both land and sea habitats. It is estimated that 4.8 to 12.7 million tons of plastic enter the ocean annually; however, the magnitude of plastic emissions on land and into freshwater systems is significantly higher, posing an even greater environmental challenge.[1] A pressing concern is the transformation of conspicuous plastic waste derived from agricultural, food, and environmental systems into microplastics (MPs, with sizes ranging from 1 μm to 5 mm) and nanoplastics (NPs, smaller than 1 μm).[2] This process of release into the environment is facilitated by mechanical stress, photochemical, thermal, and biological decomposition; processes which fracture the plastic into smaller, more pervasive fragments.[3] These particles can readily disperse into ecosystems and water bodies, potentially on exposure, leading to a variety of human health issues that involve oxidative stress, cellular damage, inflammation, DNA damage, neurotoxic effects and overall metabolic disturbances.[4,5]

Contemporary techniques for identifying and measuring MNPs typically utilize microscopic and spectroscopic approaches, such as Scanning Electron Microscopy (SEM) and Pyrolysis Mass Spectrometry (MS).[6–8] Despite the effectiveness of these procedures, significant challenges exist to increasing the efficiency of establishing a risk assessment. High costs, labor-intensive procedures, and the need for skilled operators are recognized hurdles to overcome limitations for using rapid screening techniques.[9–11] Recent advances in rapid screening applications, such as smartphone-based fluorescence microscopy and handheld surface-enhanced Raman scattering (SERS) assays, can provide fast, on-the-spot alternative methods of analysis. However, they, too, are hindered by a relatively lower sensitivity, thus reducing their applicability in real-life situations.[12,13] Our prior research reported developing a novel SERS sensor by incorporating luminescent metal-phenolic networks (L-MPNs) as Raman reporters for the rapid and sensitive detection of MPNs.[14] L-MPNs, a novel labeling strategy comprising phenolic ligands, metal ions, and conventional dyes, was successful in facilitating a rapid (<5 minutes) labeling process for various particles, such as plastics.[15] The robust Raman signals generated by the dyes used in our process allowed for serving as the Raman reporter, thereby enhancing sensitivity by up to 500 times equivalency to an unprecedentedly low detection limit of 0.1 ppm for polystyrene (PS).[14] This innovative approach has significant promise for use to assess real-world plastic contamination scenarios.

Understanding the dynamics of exposure to MNPs in the food environment is a crucial step for mitigating potential risks to human health. Such exposures can occur through skin contact, inhalation, or ingestion, including seemingly benign activities like drinking hot tea from plastic cups. Previous research has shown that the interaction of heat with plastic containers undeniably leads to the release of plastics into hot beverage fluids.[16] There is no information currently available if polyphenolics present in beverages, such as tea, for examples, have an effect on MNPs release, or can they also mute the potential adverse biological effect of MNPs. Tea catechins, particularly epigallocatechin gallate (EGCG), are present in green tea and have well-known bioactive antioxidant and anti-inflammatory activities.[17,18] In addition to tea beverages, EGCG is also found in a range of different food products packaged in plastic containers, including coffee, fruit juice, dried fruits and nuts.[19,20] The relationship between EGCG and the release of plastic particles requires further investigation to understand potential implications for human health. Moreover, we found another important use of EGCG, whereby structural characteristics showed potential use for synthesizing L-MPNs through coordination with metal ions and π-π interactions with dyes. By integrating an EGCG-based L-MPNs labeling approach with our previously developed SERS sensing platform, we can achieve in-situ monitoring of the MNPs released from plastic cups and enhance the sensitivity of MNPs detection, thus offering new insights into interactions with beneficial tea compounds that could influence subsequent health implications.

In this research, EGCG was selected not only for being a representative bioactive tea polyphenol [18], but also as a phenolic ligand candidate to form L-MPNs for SERS quantification of released plastic particles (Scheme 1). In this study, we varied factors that included the concentration of EGCG, pH and heating conditions to investigate interactions between EGCG and dynamics of plastic release. This information was expanded to determine if MNPs released posed potential cytotoxicity using the differentiated Caco-2 intestinal cell model. A second preliminary aim was to establish if the potential chemoprotective capacity of EGCG could mitigate the potential cytotoxicity of MNPs released from plastic cups exposed to heat treatments often used with tea beverages.

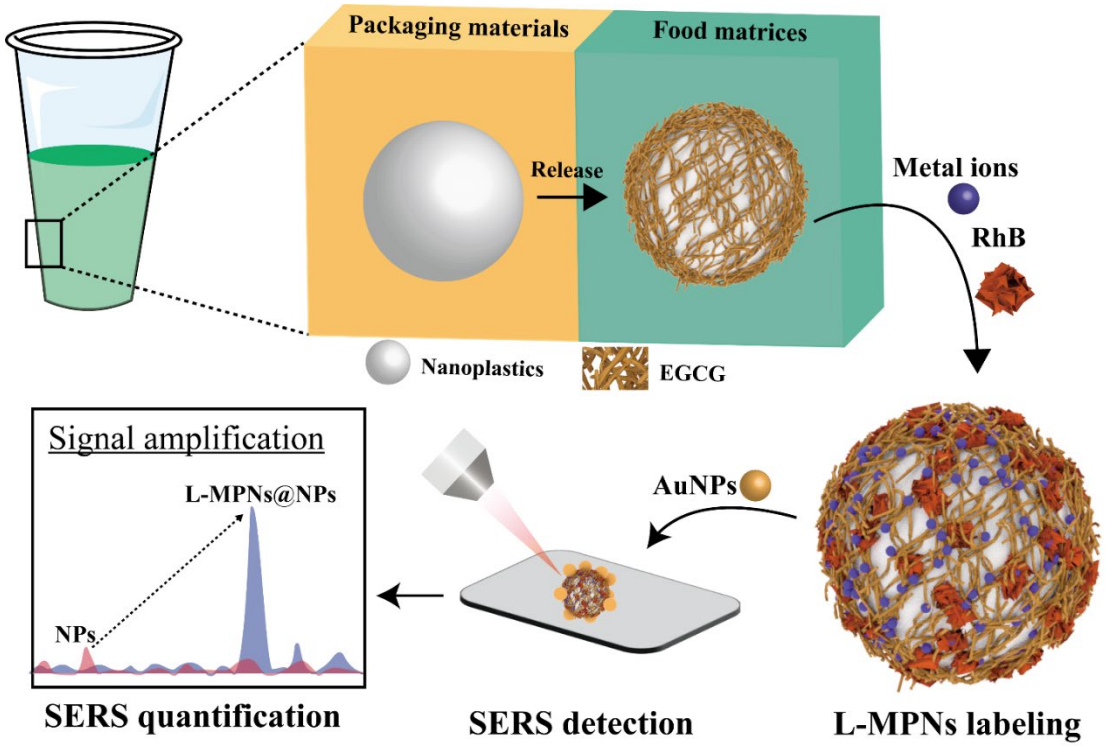

Scheme 1. Nanoplastics release and subsequent SERS detection during simulated tea drinks.

MATERIALS AND METHODS

Materials

Polystyrene nanoplastics with particle size of 500 nm were purchased from Phosphorex (Massachusetts, USA). EGCG (pharmaceutical secondary standard) and zinc chloride ($ZnCl_2$, >98%) was purchased from Sigma-Aldrich (Ontario, Canada). Rhodamine B (ACS reagent ≥99%) were purchased from VWR (Alberta, Canada). Dulbecco's Modified Eagle's Medium (DMEM-D5796; without pyruvate), phosphate buffered saline (PBS), penicillin/streptomycin antibiotics, 3-(4,5-diethylthiazol-2-yl)-2,5-diphenyltetrazolium bromide (MTT) and Dimethylsulfoxide (DMSO) were purchased from Sigma (St. Louis, MO, USA). Fetal bovine serum (FBS) was purchased from Gibco® (Grand Island, NY, USA). Transparent commercial polystyrene drinking cups (ASIN, B0B3GTSH4D) were purchased from Amazon.ca. Gold nanoparticles (AuNPs, 50 nm ± 4 nm at a concentration of 1 mg/L) were purchased from nanoComposix (San Diego, CA, USA). Double-distilled water (DD water) was produced using a distillation system in the Food Nutrition and Health building at University of British Columbia (UBC), Vancouver campus.

Preparation of L-MPNs@NPs

EGCG, Zn^{2+} metal ions, and RhB were selected as model reagents for the formation of L-MPNs. The preparation of L-MPNs labeled nanoplastics (L-MPNs@NPs) was carried out according to the protocols described in our prior research.[21] 500 nm PS NPs solutions were prepared to various concentrations of 0, 1.54×10^7, 7.7×10^7, 1.54×10^8, 7.7×10^8, 1.54×10^9, 7.7×10^9, 1.54×10^{10}, 7.7×10^{10}, 1.54×10^{11} n/mL. Subsequently, EGCG was added into these suspensions to achieve a final concentration of 1 mg/mL. For the labeling process, 20 μL of $ZnCl_2$ (20 mM) and 20 μL of RhB (0.5 mM) were added to 960 μL of NPs-EGCG mixture, resulting in final concentrations of 400 μM Zn^{2+}, and 10 μM RhB. This mixture was thoroughly vortexed for 1 min and then centrifuged at 7500 rpm for 10 min. The supernatant was removed, and the precipitate was resuspended in 1 μL of DD water to prepare L-MPNs@NPs.

Characterization of L-MPNs@NPs

L-MPNs labeling on NPs was characterized using dynamic light scattering (DLS) and fluorescence measurements. DLS assessments for released NPs and L-MPNs@NPs samples were performed with a Litesizer 500 (Anton Paar, Graz, Austria). Fluorescence spectroscopy measurements were performed with a Tecan infinite 200Pro plate reader (excitation at 550 nm; emission at 595 nm) for released NPs labeled with RhB, Zn^{2+}/RhB, EGCG/RhB and L-MPNs. Transmission Electron Microscopy (TEM) imaging was examined under a Hitachi H7600 TEM (Tokyo, Japan) at 80 kV for released NPs and NPs-EGCG mixtures.

Detection of NPs by the SERS

SERS was utilized to determine NPs labeled by L-MPNs. AuNPs solution was prepared by diluting stock solution to 0.5 mg/mL with DD water. A 1 μL droplet of AuNPs solution was applied onto aluminum foil, followed by the addition of an equal volume of the L-MPNs@NPs samples. Samples were allowed to air dry at room temperature for 10 min. Subsequently, SERS spectra were acquired at the periphery of the resultant coffee ring using a WP 785 ER Raman Spectrometer, which is equipped with a 785 nm excitation laser. The most reproducible signal from each sample was selected as the representative spectrum. Spectral acquisition was conducted under controlled conditions: the laser was set to a power of 450 mW, fixed at the integration time was 60 s, and spectra were recorded continuously over a range of 300–2008 cm^{-1}. The spectral data were processed using boxcar smoothing and polynomial baseline corrections to enhance the signal clarity for improved accuracy.

MNPs release in a simulated tea consumption

EGCG was chosen as the representative bioactive polyphenol to simulate a simple tea drink; The study utilized two primary thermal processes: boiling water and microwave heating water, with cold water control. For the boiling water treatments, different concentrations of EGCG (e.g., 0.1, 0.2, 0.4, 0.6 mg/mL) were added. In the microwave experiments, EGCG at the same concentrations used above were added to DD water at room temperature, followed by exposure to microwave heating (900 W) at varying time durations (e.g., 0, 15, 30, 60, 90, 120, 150, and 180 s). Following heating, all samples were cooled naturally at room temperature for approximately 30 min. The EGCG concentrations were adjusted to 1 mg/mL to maintain consistency across all samples. Subsequently, the release of NPs was measured by preparation of L-MPNs@NPs and then using SERS for quantification analysis.

Caco-2 cell viability exposed to NPs and NPs with EGCG.

Twenty-one day old differentiated Caco-2 cells were used in this study to test the potential toxicity of NPs recovered from the plastic cups containing hot water. Cells were cultured in Dulbecco's modified Eagle's medium (DMEM) containing 4500 mg/L glucose and sodium bicarbonate, without L-glutamine and sodium pyruvate. Cell media also contained 10% FBS (Invitrogen, Canada), and 100 U/mL penicillin and 100 µg/mL of streptomycin (PS). Cells were cultured at 37 °C under a controlled atmosphere with 5% CO_2. The passage number for Caco-2 cells used in these experiments was 21–30. Caco-2 cells were seeded in 96-well plates at a density of 1×10^5 cells/cm^2, and the cell culture media was changed every 2–3 days for 21 days until differentiation.

Redox activity was assessed in Caco-2 cells as a measure of viability using the MTT assay (3-(4,5-dimethylthiazol-2-yl)-2,5-diphenyltetrazolium bromide) in 96-well plates. This assay is based on a redox mechanism, whereby NADPH-dependent enzymes in viable, healthy cells reduce MTT into formazan crystals, which are quantified by spectrophotometry.[22] The cells were first incubated with NPs and EGCG (0.1, 0.2, 0.4, 0.6 mg/mL) in cell culture medium. A positive control consisted of using NPs (1.54×10^6, 1.54×10^7, 1.54×10^8 and 1.54×10^9 n/mL) present with no EGCG. After 24 h of incubation, Caco-2 cells were washed with 100 µL of phosphate-buffered saline (PBS) three times and then incubated with 100 µL of DMEM containing 0.5 mg/mL MTT for 4 h in the dark at 37 °C. Dimethylsulfoxide (DMSO, 100 µL) was then added to the wells without discarding the DMEM, allowing formazan crystals to dissolve (for the measuring of absorbance) with another 30 min. Solubilized formazan in wells were quantified by measuring absorbance at 540 nm, using the Multiskan Skyhigh Spectrophotometer (Thermolabsystem, Chantilly, VA, USA) with the following equation:

$$Viability\ (shown\ as\ \%\ of\ control) = \frac{Abs_{sample}}{Abs_{control}} * 100\%$$

Where Abs_{sample} = absorbance of cells that received treatment, and $Abs_{control}$ = absorbance by the cells that have not received treatment (negative control).

RESULTS AND DISCUSSION

Formation of L-MPNs@MNPs

L-MPNs labeling strategy can be applied to PS plastic particles through a straightforward and simple self-assembly process.[14] For example, in our previous research, tannic acid /zirconium metal ions/RhB-based L-MPNs was used to effectively quantify commercial 500 nm PS NPs employing SERS measurements. In this study, we used EGCG and Zn^{2+} as model reagents to form L-MPNs on released MNPs from polystyrene cups. Figure 1a depicts plastics released from commercial plastic cups subjected to microwave heating for 90 seconds. The TEM image illustrates an amorphous morphology for particle sizes ranging from the micro- to the nano- scale. Subsequent fluorescence characterization (Figure 1b) of RhB interaction with the released plastic particles showed a significant reduction in fluorescence intensity when released MNPs were labeled with RhB, EGCG/RhB, and RhB/Zn^{2+}, in comparison to the labeling with L-MPNs ($P < 0.05$). This result underscores the critical role of the L-MPNs coordination network to enhance fluorescence labeling efficiency. DLS measurements provided additional information on particle size distribution of the MNPs before and after labeling with L-MPNs. With post-labeling, there was a notable shift in the peak particle size from 307 nm to 586 nm (Figure 1c), which was indicative of successful aggregation facilitation by the L-MPNs. Although micro-sized plastic particles were detected, the predominant fraction consisted of nanoparticles in the range of hundreds of nanometers, with a maximal intensity at 586 nm. Consequently, for SERS optimization and measurement, the released plastic particles were categorized as NPs with a size distribution centered around hundreds of nanometers.

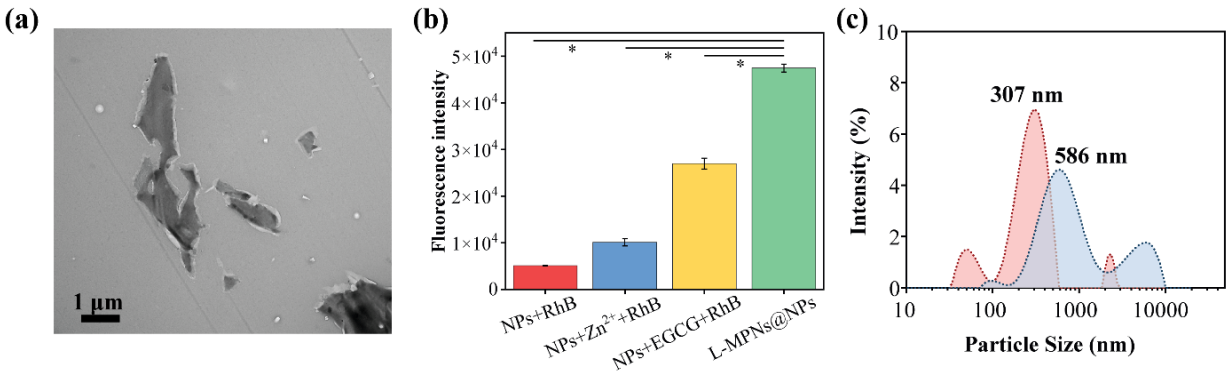

Figure 1. L-MPNs labeling of micro/nanoplastics. (a) TEM image of released plastic particles

from plastic cups with microwave heating at 90 s (b) Fluorescence intensity measurements of released plastic particles labeled with RhB, Zn^{2+}/RhB, EGCG/RhB and L-MPNs. (c) Particle size changes following the formation of L-MPNs@MNPs, in comparison to released MNPs alone. Data are presented as mean ± SD in bar charts. The asterisk (*) indicates a statistically significant difference ($P < 0.05$), as determined by the t-test.

SERS measurements of L-MPNs@NPs

To evaluate the efficacy of EGCG based L-MPNs to quantify NPs utilizing SERS techniques, a series of SERS analysis was conducted on both the components of L-MPNs and NPs, both pre- and post-labelling with L-MPNs (Figure 2a). AuNPs served as the substrate for SERS which was selected for environmental stability,[23] PS NPs (500 nm) were chosen to represent NPs according to a known particle size, which closely approximated the plastics released from PS cups as shown in Figure 1c. In the spectral analysis, AuNPs exhibited negligible signals across the spectrum. In contrast, RhB had distinctive peaks located at 1201, 1277, and 1357 cm^{-1}, respectively, with a very pronounced peak occurring at 1357 cm^{-1}, indicative of C-C stretching vibrations.[24] EGCG showed two peaks at 1340 and 1362 cm^{-1} , respectively, due to C-O vibrational modes.[25] The PS NPs displayed a characteristic peak at 998 cm^{-1}, attributed to ring-breathing modes. The synthesis of L-MPNs induced alterations in these peak patterns were due to molecular interactions between RhB, EGCG, and Zn^{2+}, and attributed to coordination bonding between EGCG and Zn^{2+} and π–π interaction between RhB and EGCG.[26] However, the prominent peak presented at 1357 cm^{-1} was maintained, which served as the characteristic peak of L-MPNs for further quantitative analysis. Upon forming L-MPNs@NPs, the characteristic peak of PS at 998 cm^{-1} was substituted by a peak from the L-MPNs with an enhanced intensity at 1357 cm^{-1}. This finding showed the effectiveness of using RhB as a Raman reporter in EGCG based L-MPNs for improving the sensitivity of SERS detection of NPs.

Subsequent experiments to optimize Zn^{2+} concentrations were conducted to determine the pivotal role of metal ions in the efficacy of L-MPNs labeling.[14] Spectral analyses of L-MPNs@NPs (500 nm PS NPs at 1.54×10^9 n/mL) with varying Zn^{2+} concentrations were based on the intensity of the characteristic peak appearing at 1357 cm^{-1} (Figure 2b). The intensity of this peak was contrasted against control signals derived from L-MPNs without NPs, thus showing the effective SERS signal attributable to the presence of NPs (Figure 2c). This optimization experiment revealed that increasing Zn^{2+} concentration produced an enhancement in peak intensity. Low Zn^{2+} concentrations (0–10 mM) were insufficient for effective L-MPNs formation on NPs, whereas higher Zn^{2+} concentrations (40–100 mM) facilitated a denser coating which facilitated greater binding activity with RhB molecules.[27] Excessive RhB binding could cause aggregation and

interfere with the optimal interaction between the RhB molecules and the SERS substrate (AuNPs), hence diminishing the SERS signal intensity. The Zn^{2+} concentration was optimized to 20 mM, as this concentration yielded the highest L-MPNs@NPs signal intensity. To ascertain the limit of detection (LOD) for NPs using this optimized EGCG based L-MPNs method, a number of SERS assays were performed across various NPs concentrations. The results indicated a limit of detection (LOD) of 7.7×10^7 particles/mL, demonstrating a statistically significant difference ($p < 0.05$) between the sample group and lower concentration groups (Figure S1). Values exceeding the LOD for SERS signal intensity showed a positive correlation with increasing NPs concentration.. A maximum concentration (1.53×10^{10}) resulted in a decrease in SERS intensity, likely due to the inhibition of the resonance Raman effect caused by aggregation.[28] Consequently, concentrations ranging from 7.7×10^7 to 7.7×10^{10} n/mL was used to establish a standard curve employing a polynomial regression model. This model has been validated for its suitability for performing quantitative analysis of NPs labeled by L-MPNs[29].

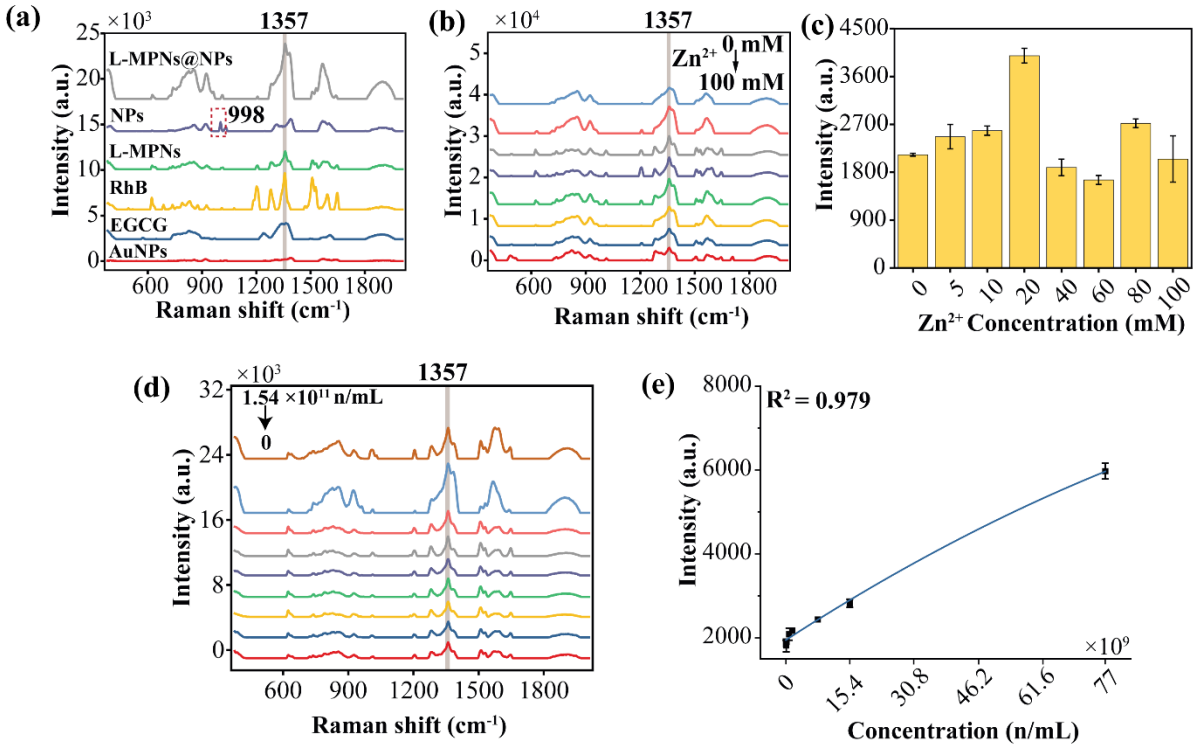

Figure 2. Optimization and Quantitative Analysis of Nanoplastics via SERS Measurements. (a) SERS spectra of AuNPs, EGCG, RhB, PS NPs, L-MPNs, and L-MPNs@NPs. (b) SERS spectra of L-MPNs@NPs with various Zn^{2+} concentrations (0, 5, 10, 20, 40, 60, 80, 100 mM). (c) Variation in the intensity of the characteristic peak at 1357 cm^{-1} for L-MPNs@NPs across these different Zn^{2+} concentrations. (d) SERS spectra of L-MPNs@NPs across various NPs concentrations (0, 1.54×10^7, 7.7×10^7, 1.54×10^8, 7.7×10^8, 1.54×10^9, 7.7×10^9, 1.54×10^{10}, 7.7×10^{10}, $1.54 \times$

10^{11} n/mL). (e) Investigation of the relationship between the concentration of NPs and the SERS characteristic peak intensity at 1357 cm^{-1} from L-MPNs employing polynomial regression model. The 500 nm PS NPs quantity concentration was controlled at 1.54×10^9 n/mL from Figure a-c. Data are presented as mean ± SD.

Nanoplastics release from PS cups containing EGCG

Release of NPs from plastic products used for hot beverages has emerged as a potential health risk in daily life.[30–32] Our study investigated NPs release from PS cups by varying the pH levels from 5 to 9 and the concentrations of EGCG, a predominant polyphenol in tea, from 0 to 0.6 mg/mL.[33] Following the application of using boiling water and water heated by microwave energy, respectively, samples were cooled and then labeled with L-MPNs before being quantified using SERS. We used EGCG in this experiment since it functioned both as a phenolic ligand, useful for the formation of L-MPNs, and also was a representative polyphenol found in tea beverages[34]. The phenolic hydroxyl groups prevalent with EGCG did not show appreciable susceptibility to oxidation when exposed to boiling water and microwave heating conditions, respectively, therefore not impacting the efficiency of L-MPNs labeling (Figure S2). We maintained a consistent EGCG concentration of 1 mg/mL across different experimental groups to ensure uniform L-MPNs labeling conditions.

We first studied the effect of EGCG concentration and pH levels on nanoplastics release during boiling water heating. Our results indicate that low concentrations of EGCG (e.g., 0.1 and 0.2 mg/mL) in cups containing boiling water result in detectable but minimal NPs release (0.5–1 $\times 10^8$ n/mL) across different pH levels. In contrast, significantly higher ($P<0.05$) NPs release (e.g., $4.26 \pm 0.32 \times 10^8$ n/mL) was observed when EGCG was present at higher concentrations (e.g., 0.4 to 0.6 mg/mL) (Figure 3a). NPs release was not detectable in cold water treatment at 30 min because the released nanoplastics are below the LOD of our sensing method (Figure S3). The ability of EGCG to facilitate NP release is attributed to the high affinity of catechol or galloyl groups in polyphenols, which can bind with various nanoplastics.[17,35] For example, electron-rich π-conjugated orbitals of aromatic rings in PS facilitate the formation of π-π interactions with polyphenol molecules. Furthermore, polyphenols rich with aromatic groups have hydrophobic interactions with various MNPs, such as PS, polyethylene (PE), polyvinyl chloride (PVC), and polypropylene (PP).[36] Under alkaline conditions (e.g., pH 9), higher concentrations of EGCG (0.6 mg/mL) resulted in more substantial NPs release compared to acidic and neutral conditions. In alkaline conditions, phenolic hydroxyl groups in polyphenols deprotonate to form phenoxide ions. The deprotonation increases the electron density on the phenoxide ion, potentially enhancing its ability to participate in π-π interactions with PS nanoplastics[37,38], thereby promoting NPs release.

TEM images confirmed the interaction between PS and EGCG, further substantiating the enhanced release of NPs (Figure 3b).

Applying microwave energy to heat water in plastic cups notably lead to higher NPs release at neutral conditions (pH 7), compared to boiling heating conditions (Figure 3a & 3c). This effect can be attributed to the susceptibility of PS polymer chains to breakdown into smaller fragments creating microcracks or fissures in the plastic cup that facilitated NPs leaching into the water.[39] The effect of EGCG to contribute to NPs release after 30-60 s exposure to microwave energy was significantly greater than the zero time control, thus denoting a significant interaction ($P<0.05$) with EGCG concentration and time of microwave heating on NPs release. Note that our SERS assay could not detect EGCG-facilitated NPs' release below LOD in control and with very short 15-second microwave heating. The greatest NPs release (e.g., $6.47 \pm 0.11 \times 10^9$ n/mL) was facilitated by the presence of EGCG occurred at 0.6 mg/mL, which also indicated that a higher concentration of EGCG induced more NPs release. The analysis of reusable cups is significant as it reflects real-world tea drinking behaviors, where individuals often refill cups multiple times. We aimed to understand the implications of such practices on NPs release. The findings indicate that reusing PS cups treated with boiling heating showed a linear increase in NPs measurements after 4 cycles, followed by a small decline thereafter (Figure 3d). Again, this was most likely due to damage to the uniform surface typical of PS cups used and exposed to repeated boiling treatments.

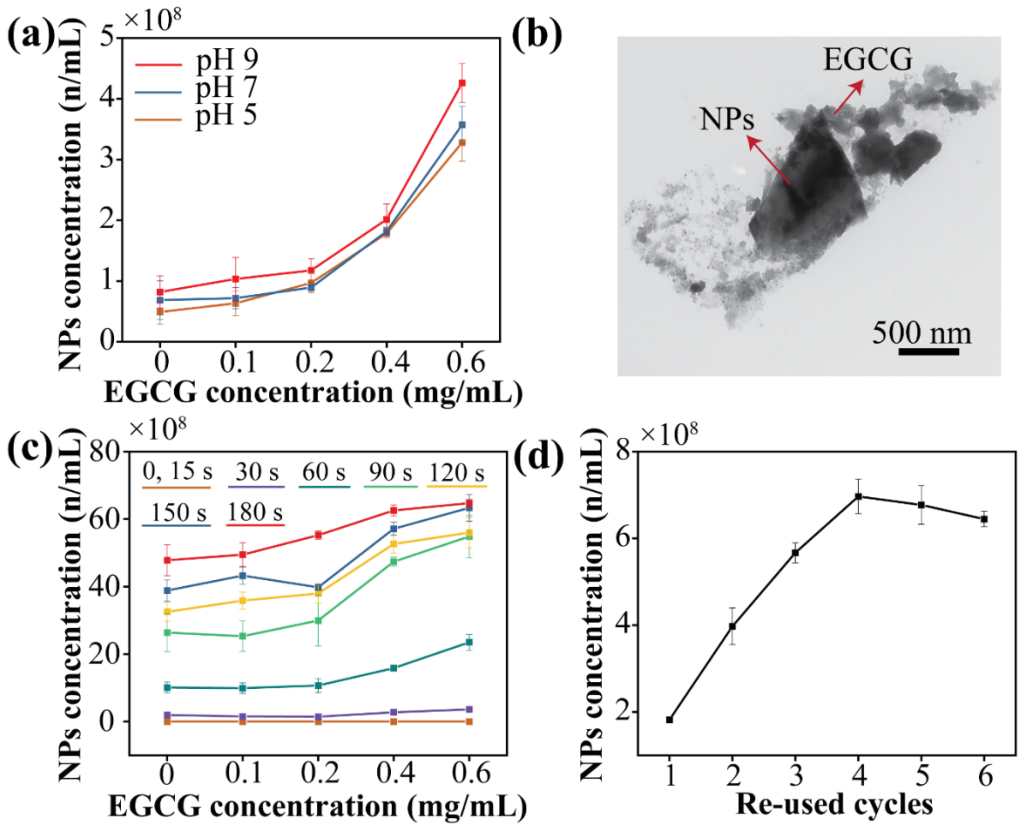

Figure 3. NPs release from water samples containing EGCG. (a) NPs release across various EGCG concentrations (0, 0.1, 0.2, 0.4, 0.6 mg/mL) and pH conditions (5, 7, 9) in boiling water. (b) TEM images of released NPs at an EGCG concentration of 0.4 mg/mL. (c) NPs release at different EGCG concentrations (0, 0.1, 0.2, 0.4, 0.6 mg/mL) subjected to various microwave heating durations (0, 15, 30, 60, 90, 120, 150, 180 s). (d) NPs release over various reuse cycles. Data are represented as mean ± SD. No detectable NPs were recovered from cold water treatments.

Caco-2 cell cytotoxicity

Differentiated Caco-2 cells served as a representative *in vitro* model for the human intestinal epithelium, enabling the evaluation of the cytotoxic potential of NPs. In this study, we employed changes in Caco-2 cell redox status to assess cell viability when exposed to NPs derived from 500 nm PS. Our findings in Figure 4a indicate that low NPs concentrations (1.54×10^7 and 1.54×10^6 n/mL) do not significantly alter cell viability from 100% MTT control. Conversely, higher PS nanoplastic concentrations (e.g., 1.54×10^8 and 1.54×10^9 n/mL), decreased viability to 91.46 ± 3.02% and 82.09 ± 2.39%, respectively ($P<0.05$). These results corroborate previous findings that reported elevated concentrations of NPs are cytotoxic to Caco-2 cells[40], through mechanisms that are associated with oxidative stress, inflammatory responses, and disruption of cellular functions.[41]

The very small size of NPs likely facilitates penetration and accumulation within cellular structures, exacerbating a toxic effect. Examining the effect of pH (e.g., 5-9) on the toxicity of released NPs exposed to microwave heating (90 s) and boiling conditions showed that pH was not a factor in increasing toxicity of NPs. (Figure 4b). Comparing microwave heating with direct heat boiling showed that the former resulted in a greater release of NPs ($P<0.05$) and, thus, higher cytotoxicity.

We also explored the potential beneficial effects of adding tea polyphenol, EGCG to potentially reduce Caco-2 cell toxicity during microwave heating and boiling conditions, respectively. Increasing EGCG concentrations significantly enhanced cell MTT responses ($P<0.05$) under these two heating conditions (Figure 4c). EGCG is a known antioxidant with the capacity to scavenge reactive oxygen species, inhibit pro-oxidant enzymes, and activate endogenous antioxidant enzyme mechanisms such as superoxide dismutase and catalase.[42] When PS cups were microwaved, NPs release in heated water occurred and EGCG at low concentrations (0.1 mg/mL) were insufficient to mitigate the cytotoxic effects induced by NPs. However, at higher concentrations of EGCG (0.2, 0.4, 0.6 mg/mL), reduced Caco-2 cell toxicity was replaced to above 100% of control. In contrast with boiling water, where NP release was low, the toxic impact on intestinal cells was also minimal. Thus, EGCG showed a beneficial effect in reducing toxicity overall concentrations. These observations underscore the importance of accounting for both the source of plastic exposure and the presence of polyphenolic compounds when assessing the effect of using microwave heating on tea beverages.

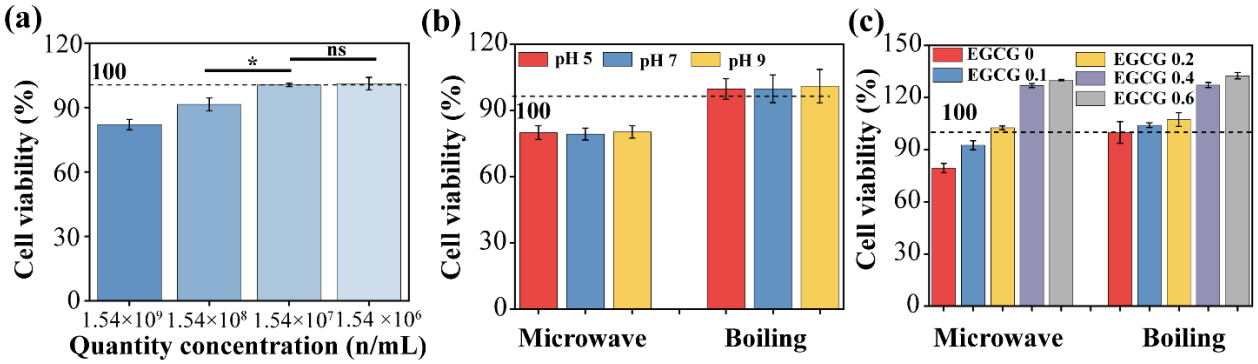

Figure 4. Influence of PS NPs and EGCG on the viability of Caco-2 cells. (a) Cell viability following exposure to commercially 500 nm PS NPs at concentrations of 1.54×10^6, 1.54×10^7, 1.54×10^8, and 1.54×10^9/mL. (b) Cell viability following exposure to released NPs at different pH levels (5, 7, 9) under microwave heating and boiling conditions. (c) Cell viability following exposure to released NPs at different EGCG levels (0, 0.1, 0.2, 0.4, 0.6 mg/mL) under microwave heating and boiling conditions. Data are represented as mean ± SD of three technical replicates. Values were determined when comparing with cold water control (100%). The label "ns" denotes

no significant difference, whereas the asterisk "*" signifies a statistically significant difference with a p-value < 0.05, as determined by the t-test.

In conclusion, our study reports on the ability to make accurate quantitative measurements of PS nanoparticles that are released when cups contain polyphenols during heating treatments. We demonstrated that beverage ingredient EGCG can increase nanoplastic release possibly due to the interaction of PS nanoplastics with EGCG that could drive more nanoplastics release. In addition, we highlight the interplay between beverage components, packaging materials, and environmental factors that may influence consumer health. Our findings, therefore, advocate for a systemic reevaluation of food packaging materials that are exposed to thermal processing, especially microwave heating, and the benefits of consuming beverages that contain polyphenol antioxidants, such as EGCG, to mitigate the risk of nanoplastics.

ASSOCIATED CONTENT

The Supporting Information is available free of charge.

Effect of heating on SERS detection, SERS detection of nanoplastics (PDF)

AUTHOR INFORMATION

Corresponding Author

***E-mail:tianxi.yang@ubc.ca**

Present Addresses

Food, Nutrition and Health, Faculty of Land and Food Systems, The University of British Columbia, 2205 East Mall, Vancouver BC, V6T 1Z4 Canada

Author Contributions

The manuscript was written through contributions of all authors. All authors have given approval to the final version of the manuscript.

Notes

The authors declare no competing financial interest.

ACKNOWLEDGMENT

This work was supported by the UBC Faculty of Land and Food Systems/Start Up Funds (AWD-020249 UBCLANDF 2022), Natural Sciences and Engineering Research Council of Canada (NSERC) Discovery Grants Program (RGPIN-2023-04100) and NSERC Discovery

Grants Program-Discovery Launch Supplement (DGECR-2023-00386). We acknowledge the Canada Foundation for Innovation and John R. Evans Leaders Fund (CFI-JELF #44768), and the British Columbia Knowledge Development Fund (BCKDF). We also thank V. Pringle from the UBC Bioimaging Facility (RRID: SCR_021304) for completing TEM.

References

(1) Li, W.; Wu, C.; Xiong, Z.; Liang, C.; Li, Z.; Liu, B.; Cao, Q.; Wang, J.; Tang, J.; Li, D. Self-Driven Magnetorobots for Recyclable and Scalable Micro/Nanoplastic Removal from Nonmarine Waters. *Science Advances* **2022**, *8* (45), eade1731. https://doi.org/10.1126/sciadv.ade1731.

(2) Ye, H.; Zheng, X.; Yang, H.; Kowal, M.; Seifried, T.; Singh, G. P.; Aayush, K.; Gao, G.; Grant, E.; Kitts, D.; Yada, R.; Yang, T. Rapid Detection of Micro/Nanoplastics Via Integration of Luminescent Metal Phenolic Networks Labeling and Quantitative Fluorescence Imaging in A Portable Device. ChemRxiv September 29, 2023. https://doi.org/10.26434/chemrxiv-2023-jnbm1.

(3) Stubbins, A.; Law, K. L.; Muñoz, S. E.; Bianchi, T. S.; Zhu, L. Plastics in the Earth System. *Science* **2021**, *373* (6550), 51–55. https://doi.org/10.1126/science.abb0354.

(4) Yin, K.; Wang, Y.; Zhao, H.; Wang, D.; Guo, M.; Mu, M.; Liu, Y.; Nie, X.; Li, B.; Li, J.; Xing, M. A Comparative Review of Microplastics and Nanoplastics: Toxicity Hazards on Digestive, Reproductive and Nervous System. *Science of The Total Environment* **2021**, *774*, 145758. https://doi.org/10.1016/j.scitotenv.2021.145758.

(5) Hu, M.; Palić, D. Micro- and Nano-Plastics Activation of Oxidative and Inflammatory Adverse Outcome Pathways. *Redox Biology* **2020**, *37*, 101620. https://doi.org/10.1016/j.redox.2020.101620.

(6) Fang, C.; Luo, Y.; Naidu, R. Microplastics and Nanoplastics Analysis: Options, Imaging, Advancements and Challenges. *TrAC Trends in Analytical Chemistry* **2023**, *166*, 117158. https://doi.org/10.1016/j.trac.2023.117158.

(7) Shi, K.; Zhang, H.; Yang, Y.; Huang, Y.; Gao, J.; Zhang, J.; Kan, G.; Jiang, Y.; Jiang, J. Efficient Extraction and Analysis of Nanoplastics by Ionic Liquid-Assisted Cloud-Point Extraction Coupled with Electromagnetic Heating Pyrolysis Mass Spectrometry. *Anal. Chem.* **2024**. https://doi.org/10.1021/acs.analchem.3c05208.

(8) Cai, H.; Xu, E. G.; Du, F.; Li, R.; Liu, J.; Shi, H. Analysis of Environmental Nanoplastics: Progress and Challenges. *Chemical Engineering Journal* **2021**, *410*, 128208. https://doi.org/10.1016/j.cej.2020.128208.

(9) Zhang, X.; Shi, K.; Liu, Y.; Chen, Y.; Yu, K.; Wang, Y.; Zhang, H.; Jiang, J. Rapid and Efficient Method for Assessing Nanoplastics by an Electromagnetic Heating Pyrolysis Mass Spectrometry. *Journal of Hazardous Materials* **2021**, *419*, 126506. https://doi.org/10.1016/j.jhazmat.2021.126506.

(10) Xiang, C.; Gao, J.; Ye, H.; Ren, G.; Ma, X.; Xie, H.; Fang, S.; Lei, Q.; Fang, W. Development of Ovalbumin-Pectin Nanocomplexes for Vitamin D3 Encapsulation: Enhanced Storage

Stability and Sustained Release in Simulated Gastrointestinal Digestion. *Food Hydrocolloids* **2020**, *106*, 105926. https://doi.org/10.1016/j.foodhyd.2020.105926.

(11) Ye, H.; Chen, T.; Huang, M.; Ren, G.; Lei, Q.; Fang, W.; Xie, H. Exploration of the Microstructure and Rheological Properties of Sodium Alginate-Pectin-Whey Protein Isolate Stabilized B-Carotene Emulsions: To Improve Stability and Achieve Gastrointestinal Sustained Release. *Foods* **2021**, *10* (9), 1991. https://doi.org/10.3390/foods10091991.

(12) Li, Z.; Han, K.; Zhang, A.; Wang, T.; Yan, Z.; Ding, Z.; Shen, Y.; Zhang, M.; Zhang, W. Honeycomb-like AgNPs@TiO2 Array SERS Sensor for the Quantification of Micro/Nanoplastics in the Environmental Water Samples. *Talanta* **2024**, *266*, 125070. https://doi.org/10.1016/j.talanta.2023.125070.

(13) Leonard, J.; Koydemir, H. C.; Koutnik, V. S.; Tseng, D.; Ozcan, A.; Mohanty, S. K. Smartphone-Enabled Rapid Quantification of Microplastics. *Journal of Hazardous Materials Letters* **2022**, *3*, 100052. https://doi.org/10.1016/j.hazl.2022.100052.

(14) Ye, H.; Gao, G.; Yang, T. Quantitative and Rapid Detection of Nanoplastics Labeled by Luminescent Metal Phenolic Networks Using Surface Enhanced Raman Scattering. Rochester, NY January 26, 2024. https://doi.org/10.2139/ssrn.4696808.

(15) Lin, Z.; Zhou, J.; Qu, Y.; Pan, S.; Han, Y.; Lafleur, R. P. M.; Chen, J.; Cortez-Jugo, C.; Richardson, J. J.; Caruso, F. Luminescent Metal-Phenolic Networks for Multicolor Particle Labeling. *Angewandte Chemie International Edition* **2021**, *60* (47), 24968–24975. https://doi.org/10.1002/anie.202108671.

(16) Hernandez, L. M.; Xu, E. G.; Larsson, H. C. E.; Tahara, R.; Maisuria, V. B.; Tufenkji, N. Plastic Teabags Release Billions of Microparticles and Nanoparticles into Tea. *Environ. Sci. Technol.* **2019**, *53* (21), 12300–12310. https://doi.org/10.1021/acs.est.9b02540.

(17) Xie, H.; Luo, X.; Gao, Y.; Huang, M.; Ren, G.; Zhou, R.; Sun, Y.; Ye, H.; Lei, Q.; Fang, W.; Xu, Y.-Q. Co-Encapsulation of *Lactobacillus Plantarum* and EGCG: A Promising Strategy to Increase the Stability and Lipid-Lowering Activity. *Food Hydrocolloids* **2024**, *151*, 109768. https://doi.org/10.1016/j.foodhyd.2024.109768.

(18) Hu, C.; Kitts, D. D. Evaluation of Antioxidant Activity of Epigallocatechin Gallate in Biphasic Model Systems in Vitro. *Mol Cell Biochem* **2001**, *218* (1), 147–155. https://doi.org/10.1023/A:1007220928446.

(19) Arts, I. C. W.; van de Putte, B.; Hollman, P. C. H. Catechin Contents of Foods Commonly Consumed in The Netherlands. 2. Tea, Wine, Fruit Juices, and Chocolate Milk. *J. Agric. Food Chem.* **2000**, *48* (5), 1752–1757. https://doi.org/10.1021/jf000026+.

(20) Atanasov, A. G.; Sabharanjak, S. M.; Zengin, G.; Mollica, A.; Szostak, A.; Simirgiotis, M.; Huminiecki, Ł.; Horbanczuk, O. K.; Nabavi, S. M.; Mocan, A. Pecan Nuts: A Review of Reported Bioactivities and Health Effects. *Trends in Food Science & Technology* **2018**, *71*, 246–257. https://doi.org/10.1016/j.tifs.2017.10.019.

(21) Ye, H.; Esfahani, E. B.; Chiu, I.; Mohseni, M.; Gao, G.; Yang, T. Quantitative and Rapid Detection of Nanoplastics Labeled by Luminescent Metal Phenolic Networks Using Surface-Enhanced Raman Scattering. *Journal of Hazardous Materials* **2024**, *470*, 134194. https://doi.org/10.1016/j.jhazmat.2024.134194.

(22) Kumar, P.; Nagarajan, A.; Uchil, P. D. Analysis of Cell Viability by the MTT Assay. *Cold Spring Harb Protoc* **2018**, *2018* (6), pdb.prot095505. https://doi.org/10.1101/pdb.prot095505.
(23) Wu, L.-A.; Li, W.-E.; Lin, D.-Z.; Chen, Y.-F. Three-Dimensional SERS Substrates Formed with Plasmonic Core-Satellite Nanostructures. *Sci Rep* **2017**, *7* (1), 13066. https://doi.org/10.1038/s41598-017-13577-9.
(24) Huh, S.; Park, J.; Kim, Y. S.; Kim, K. S.; Hong, B. H.; Nam, J.-M. UV/Ozone-Oxidized Large-Scale Graphene Platform with Large Chemical Enhancement in Surface-Enhanced Raman Scattering. *ACS Nano* **2011**, *5* (12), 9799–9806. https://doi.org/10.1021/nn204156n.
(25) Zhao, Y.; Xu, L.; Kong, F.; Yu, L. Design and Preparation of Poly(Tannic Acid) Nanoparticles with Intrinsic Fluorescence: A Sensitive Detector of Picric Acid. *Chemical Engineering Journal* **2021**, *416*, 129090. https://doi.org/10.1016/j.cej.2021.129090.
(26) Lin, Z.; Zhou, J.; Qu, Y.; Pan, S.; Han, Y.; Lafleur, R. P. M.; Chen, J.; Cortez-Jugo, C.; Richardson, J. J.; Caruso, F. Luminescent Metal-Phenolic Networks for Multicolor Particle Labeling. *Angewandte Chemie International Edition* **2021**, *60* (47), 24968–24975. https://doi.org/10.1002/anie.202108671.
(27) Mazaheri, O.; Alivand, M. S.; Zavabeti, A.; Spoljaric, S.; Pan, S.; Chen, D.; Caruso, F.; Suter, H. C.; Mumford, K. A. Assembly of Metal–Phenolic Networks on Water-Soluble Substrates in Nonaqueous Media. *Advanced Functional Materials* **2022**, *32* (24), 2111942. https://doi.org/10.1002/adfm.202111942.
(28) Bell, S. E. J.; Sirimuthu, N. M. S. Quantitative Surface-Enhanced Raman Spectroscopy. *Chem. Soc. Rev.* **2008**, *37* (5), 1012. https://doi.org/10.1039/b705965p.
(29) Ye, H.; Jiang, S.; Yan, Y.; Zhao, B.; Grant, E.; Kitts, D.; Yada, R.; Pratap-Singh, A.; Baldelli, A.; Yang, T. Integrating Metal Phenolic Networks-Mediated Separation and Machine Learning-Aided SERS for High-Precision Quantification and Classification of Nanoplastics. ChemRxiv July 5, 2024. https://doi.org/10.26434/chemrxiv-2024-kn4zj.
(30) Liu, G.; Wang, J.; Wang, M.; Ying, R.; Li, X.; Hu, Z.; Zhang, Y. Disposable Plastic Materials Release Microplastics and Harmful Substances in Hot Water. *Science of The Total Environment* **2022**, *818*, 151685. https://doi.org/10.1016/j.scitotenv.2021.151685.
(31) Hernandez, L. M.; Xu, E. G.; Larsson, H. C. E.; Tahara, R.; Maisuria, V. B.; Tufenkji, N. Plastic Teabags Release Billions of Microparticles and Nanoparticles into Tea. *Environ. Sci. Technol.* **2019**, *53* (21), 12300–12310. https://doi.org/10.1021/acs.est.9b02540.
(32) Hee, Y. Y.; Weston, K.; Suratman, S. The Effect of Storage Conditions and Washing on Microplastic Release from Food and Drink Containers. *Food Packaging and Shelf Life* **2022**, *32*, 100826. https://doi.org/10.1016/j.fpsl.2022.100826.
(33) Zhen-Yu Chen, *; Qin Yan Zhu, †; David Tsang, † and; Huang‡, Y. *Degradation of Green Tea Catechins in Tea Drinks*. ACS Publications. https://doi.org/10.1021/jf000877h.
(34) Xie, H.; Luo, X.; Gao, Y.; Huang, M.; Ren, G.; Zhou, R.; Sun, Y.; Ye, H.; Lei, Q.; Fang, W.; Xu, Y.-Q. Co-Encapsulation of *Lactobacillus Plantarum* and EGCG: A Promising Strategy to Increase the Stability and Lipid-Lowering Activity. *Food Hydrocolloids* **2024**, *151*, 109768. https://doi.org/10.1016/j.foodhyd.2024.109768.
(35) Zhao, W.; Liang, X.; Wang, X.; Wang, S.; Wang, L.; Jiang, Y. Chitosan Based Film

Reinforced with EGCG Loaded Melanin-like Nanocomposite (EGCG@MNPs) for Active Food Packaging. *Carbohydrate Polymers* **2022**, *290*, 119471. https://doi.org/10.1016/j.carbpol.2022.119471.

(36) Wang, Y.; Wang, M.; Wang, Q.; Wang, T.; Zhou, Z.; Mehling, M.; Guo, T.; Zou, H.; Xiao, X.; He, Y.; Wang, X.; Rojas, O. J.; Guo, J. Flowthrough Capture of Microplastics through Polyphenol-Mediated Interfacial Interactions on Wood Sawdust. *Advanced Materials* **2023**, *35* (36), 2301531. https://doi.org/10.1002/adma.202301531.

(37) Zhu, H.; Ma, X.; Kong, J. Y.; Zhang, M.; Kenttämaa, H. I. Identification of Carboxylate, Phosphate, and Phenoxide Functionalities in Deprotonated Molecules Related to Drug Metabolites via Ion–Molecule Reactions with Water and Diethylhydroxyborane. *J. Am. Soc. Mass Spectrom.* **2017**, *28* (10), 2189–2200. https://doi.org/10.1007/s13361-017-1713-0.

(38) Zhang, L.; Liu, Y.; Wang, Y. Deprotonation Mechanism of Methyl Gallate: UV Spectroscopic and Computational Studies. *International Journal of Molecular Sciences* **2018**, *19* (10), 3111. https://doi.org/10.3390/ijms19103111.

(39) Awaja, F.; Zhang, S.; Tripathi, M.; Nikiforov, A.; Pugno, N. Cracks, Microcracks and Fracture in Polymer Structures: Formation, Detection, Autonomic Repair. *Progress in Materials Science* **2016**, *83*, 536–573. https://doi.org/10.1016/j.pmatsci.2016.07.007.

(40) Xu, D.; Ma, Y.; Han, X.; Chen, Y. Systematic Toxicity Evaluation of Polystyrene Nanoplastics on Mice and Molecular Mechanism Investigation about Their Internalization into Caco-2 Cells. *Journal of Hazardous Materials* **2021**, *417*, 126092. https://doi.org/10.1016/j.jhazmat.2021.126092.

(41) Llorca, M.; Farré, M. Current Insights into Potential Effects of Micro-Nanoplastics on Human Health by in-Vitro Tests. *Front. Toxicol.* **2021**, *3*. https://doi.org/10.3389/ftox.2021.752140.

(42) Mattioda, V.; Benedetti, V.; Tessarolo, C.; Oberto, F.; Favole, A.; Gallo, M.; Martelli, W.; Crescio, M. I.; Berio, E.; Masoero, L.; Benedetto, A.; Pezzolato, M.; Bozzetta, E.; Grattarola, C.; Casalone, C.; Corona, C.; Giorda, F. Pro-Inflammatory and Cytotoxic Effects of Polystyrene Microplastics on Human and Murine Intestinal Cell Lines. *Biomolecules* **2023**, *13* (1), 140. https://doi.org/10.3390/biom13010140.

535

536

Table of Content

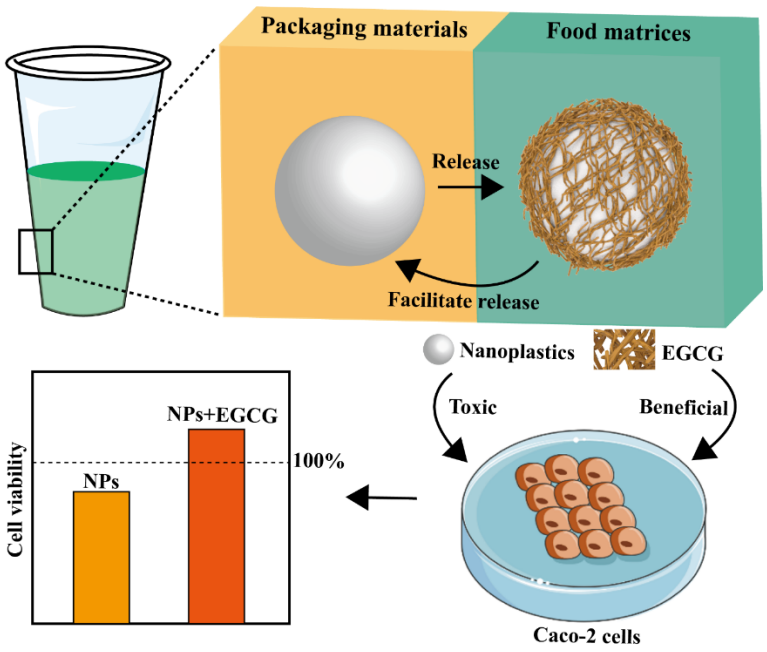

537